

Causality on Cross-Sectional Data: Stable Specification Search in Constrained Structural Equation Modeling

Ridho Rahmadi, Perry Groot, Marianne Heins,
Hans Knoop, Tom Heskes, The OPTIMISTIC consortium*

Abstract—Causal modeling has long been an attractive topic for many researchers and in recent decades there has seen a surge in theoretical development and discovery algorithms. Generally discovery algorithms can be divided into two approaches: constraint-based and score-based. A disadvantage of currently existing constraint-based and score-based approaches, however, is the inherent instability in structure estimation. With finite samples small changes in the data can lead to completely different optimal structures. The present work introduces a new score-based causal discovery algorithm that is robust for finite samples based on recent advances in stability selection using subsampling and selection algorithms. Structure search is performed over Structural Equation Models. Our approach uses exploratory search but allows incorporation of prior background knowledge to constrain the search space. We show that our approach produces accurate structure estimates on one simulated data set and two real-world data sets for Chronic Fatigue Syndrome and Attention Deficit Hyperactivity Disorder.

Index Terms—Causal modeling, Structural equation model, Stability selection, Multi-objective evolutionary algorithm.



1 INTRODUCTION

CAUSAL modeling has been an attractive topic for many researchers for decades. Especially since the 1990s there has been an enormous increase in theoretical development, partly because of advances in graphical modeling [2]. This has led to a variety of causal discovery algorithms in the literature. In general, discovery algorithms can be divided into two approaches: constraint-based and score-based. Constraint-based approaches work with conditional independence tests. First, they construct a skeleton graph starting with the complete graph and excluding edges between variables

that are conditionally independent. Second, edges are oriented to arrive at a causal graph. Examples of constraint-based approaches are the IC algorithm [3], PC-FCI [4], and TC [5]. Score-based approaches assign scores to particular graph structures based on the data fit and the complexity of the graph. Different scoring metrics that are often used are the Bayesian score [6] and the BIC score [7]. The goal of the score-based approach is to find the graph structure with the highest score. This optimization problem is, however, NP-hard thus different search heuristics are often used. The approach advocated in this paper is an example of a score-based approach.

A disadvantage of both score-based and constrained-based approaches, however, is the inherent instability in structure estimation. With finite samples small changes in the data can lead to completely different optimal structures. Outcomes of borderline independence tests can be incorrect and can lead to multiple errors when propagated by the discovery algorithm [8]. Some conservative algorithms such

- R. Rahmadi is with the Department of Informatics, Universitas Islam Indonesia and Institute for Computing and Information Sciences, Radboud University Nijmegen, the Netherlands. E-mail: r.rahmadi@cs.ru.nl
- P. Groot and T. Heskes are with Institute for Computing and Information Sciences, Radboud University Nijmegen, the Netherlands.
- M. Heins and H. Knoop are with Expert Centre for Chronic Fatigue, Radboud University Medical Centre, the Netherlands.
- *The members of OPTIMISTIC consortium are described in [1].

as CPC [9] and CFCI [10] have been developed, which are more robust but also produce less informative structures.

The present work introduces a new score-based causal discovery algorithm that is robust for finite samples based on advances in stability selection using subsampling and selection algorithms. Structure search is performed over Structural Equation Models (SEM), which is the most widely used language for causal discovery in various scientific disciplines. The method uses exploratory search, but allows incorporation of prior background knowledge to constrain the search space. We show that our approach produces accurate structure estimates on one simulated data set and two real-world data sets for Chronic Fatigue Syndrome and Attention Deficit Hyperactivity Disorder.

The rest of this paper is structured as follows. Section 2 describes all the background material obtained from the existing literature. Section 3 describes our robust score-based approach for causal discovery. Section 4 presents experimental result on one simulated and two real-world data sets. Section 5 gives conclusions and suggestions for future work.

2 BACKGROUND

2.1 Directed Acyclic Graph

We first describe some graphical notation and terminology used in the remaining sections. A graph is a pair (V, E) with V a set of nodes and E a set of edges. A *directed graph* has all edges in E directed (arc); a single arrowhead on every edge, e.g., $A \rightarrow B$. Directed cycles represent feedback or reciprocal relationships, e.g., $A \rightarrow B \rightarrow A$. A graph with no directed cycles is called *acyclic*. A graph which is both directed and acyclic is called a *Directed Acyclic Graph* (DAG) [2]. Figure 1 depicts a DAG of four variables. The *skeleton* of a DAG is the undirected graph that results from removing the directionality of every edge. A *v-structure* in a DAG G is an ordered triple (x, y, z) such that G contains the directed edges $x \rightarrow y$, $z \rightarrow y$, and x and z are not adjacent in G [11].

2.2 Causal Modeling in SEM

In this study, we focus on causal models with no reciprocal or feedback relationships, and no latent variables. Generally, there are two common ways of representing a model in SEM: by stating all relations in the set as equations, which is called a *causal model*, or by drawing them as a *causal diagram* (graph). The general form of the equations is

$$x_i = f_i(\text{pa}_i, \varepsilon_i), \quad i = 1, \dots, n.$$

where pa_i denotes the *parents* which represent the set of variables considered to be direct causes of X_i and ε_i represents errors on account of omitted factors that are assumed to be mutually independent [2].

2.3 Specification Search in SEM

Typically, a SEM is used as follows: 1) set a hypothesis as the prior model, 2) fit the model to the data, 3) evaluate the model, and 4) modify the model to improve the parsimony and score [12]. The last step is called *specification search* [13], [14]. This typical model refinement approach is hypothesis-driven. It works by adding or deleting some arcs between variables from the initial model. Typically only a few models are evaluated, making it difficult to derive causal relationships.

An alternative approach is exploratory search in which no prior hypothesis is specified. Typical approaches in the literature for addressing the exponential search space include tabu search [15], genetic algorithms [16], [17], ant colony optimization [18], and others [19], [20], [21].

2.4 Multi-objective Optimization

Following the principle of Occam's razor, we should prefer models that are simple and fit the

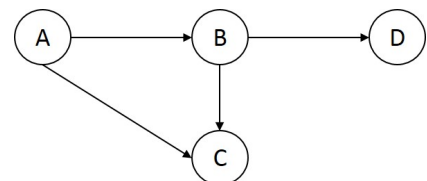


Fig. 1: DAG of four variables.

data well. These two objectives, however, are often conflicting as a well-fit model is likely to be a complex model. In this paper, we propose to make use of multi-objective optimization to explicitly optimize both objectives.

In multi-objective optimization, optimal solutions are defined in terms of *domination*. A model \mathbf{x}_1 is said to dominate model \mathbf{x}_2 , if the following conditions are satisfied [22]:

$$\mathbf{x}_1 \preceq \mathbf{x}_2 \text{ iff } \begin{cases} \forall i \in \{1, \dots, M\} & f_i(\mathbf{x}_1) \leq f_i(\mathbf{x}_2) \\ \exists j \in \{1, \dots, M\} & f_j(\mathbf{x}_1) < f_j(\mathbf{x}_2) \end{cases}$$

The first condition states that the model \mathbf{x}_1 is no worse than \mathbf{x}_2 in all objectives f_i . The second condition states that the model \mathbf{x}_1 is strictly better than \mathbf{x}_2 in at least one objective. By using this concept, given the population of models P , we can partition P into n sets called *fronts* F_1, \dots, F_n , such that F_k dominates F_l where $1 \leq k < l \leq n$ and the models within the same front do not dominate each other. The so-called *Pareto Front* or *non-dominated set* F_1 includes models that are not dominated by any member of P . Figure 2 provides a sketch.

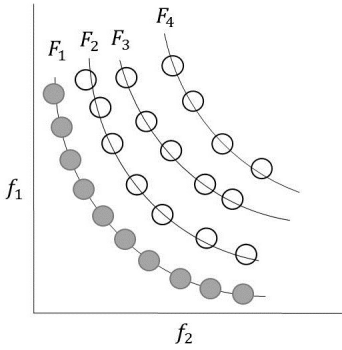


Fig. 2: Example of a population P partitioned into fronts F_1, \dots, F_n when minimizing objectives f_1 and f_2 . F_1 is the Pareto front not dominated by any member of P .

2.4.1 NSGA-II

Non-dominated Sorting Genetic Algorithm II or NSGA-II [23] is a well-known Multi-objective evolutionary algorithm (MOEA), which contains several clever procedures. The first characteristic feature is *fast non-dominated sorting* which sorts models based on the concept of domination. With M the number of

objectives and N the size of population, the time complexity has order $\mathcal{O}(MN^2)$, which is better than a naïve approach with $\mathcal{O}(MN^3)$. The second characteristic feature is *crowding distance sorting* which is implemented to preserve the diversity among the solutions in the Pareto front. This feature sorts models based on the distance metric which explains the proximity of a model to other models. NSGA-II has been developed to improve upon NSGA, which has problems such as time complexity of the sorting algorithm, lack of elitism (best solution of a generation), and the need for sharing parameters.

The iterative procedure of NSGA-II shown in Figure 3 is a sequence of steps started by generating a population of solutions P of size N . P is then manipulated by genetic operators such as selection, crossover, and mutation, forming a new population Q of size N . P and Q are then combined into population R with size $2N$. After that R is sorted using fast non-dominated sorting, yielding a set of fronts F . In the next iteration each front in F is sorted using the crowding distance sorting and the first N members are used to generate a new population P . At $t = 0$, P is formed by creating N random solutions sorted with fast non-dominated sorting.

2.5 Stability Selection

Structure estimation is a notoriously difficult problem, both because of computational aspects (finding the optimal structure can be NP hard) and because of instability (small changes in the data can lead to completely different optimal structures). In this section we describe the method of [24] for robust estimation of model structure based on subsampling in combination with selection algorithms. The method has been shown to yield finite sample family wise error control and improved structure estimates.

Let β be a sparse p -dimensional vector which is a general representation for, for example, the coefficient vector in linear regression or for the edges in a graph. In structure estimation the goal is to infer the set $S = \{k : \beta_k \neq 0\}$ of non-zero components from noisy observations. Many methods tackle this problem by minimizing some loss function augmented with a

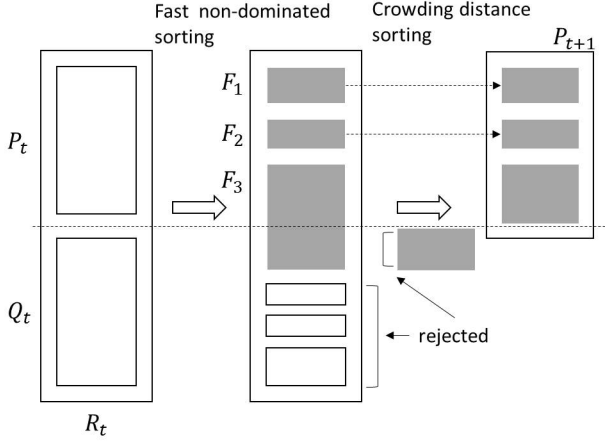


Fig. 3: Adopted from [23]. P is the current population with size N and is manipulated to make a new population Q . Both are combined, forming R , which will be sorted using fast non-dominated yielding a set of fronts F . Every member of front $F_n \in F$ will be assigned a so-called crowding distance in order to sort F_k . The first N members of F will be selected to be the next population P .

regularization term to avoid overfitting. Usually the regularization term is parameterized by $\lambda \in \Lambda \subseteq \mathbb{R}^+$ and each λ leads to an estimated structure $\hat{S}^\lambda \subseteq \{1, \dots, p\}$. The objective is to determine λ such that \hat{S}^λ is identical to S with high probability. To this end, [24] introduces the concepts of *selection probabilities* and *stability paths*.

Definition 1 (Selection probabilities). *Let I be a subset of $\{1, \dots, n\}$ of size $\lfloor n/2 \rfloor$ randomly drawn without replacement, $K \subseteq \{1, \dots, p\}$, and $\hat{S}^\lambda(I)$ be the selected set \hat{S}^λ for subsample I . The probability of K being in set $\hat{S}^\lambda(I)$ is*

$$\hat{\Pi}_K^\lambda = P(K \subseteq \hat{S}^\lambda(I))$$

where the probability being is with respect to the random subsampling and possibly the construction of $\hat{S}^\lambda(I)$.

Definition 2 (Stability path). *For each variable $k = 1, \dots, p$ the stability path is given by the selection probabilities $\{\hat{\Pi}_k^\lambda : \lambda \in \Lambda\}$.*

Furthermore, in stability selection we do not select a single element from the set of models $\{\hat{S}^\lambda : \lambda \in \Lambda\}$ as traditional methods do, but

perturb the data many times and select structures or variables that occur in a large fraction of selected sets. To this end, [10] introduces the concept of *stable variables*.

Definition 3 (Stable variables). *The set of stable variables is defined as*

$$\hat{S}^{stable} = \{k : \max_{\lambda \in \Lambda} \hat{\Pi}_k^\lambda \geq \pi_{thr}\}$$

where π_{thr} is a cutoff with $0 < \pi_{thr} < 1$.

Variables with a high selection probability are kept whereas those with low selection probabilities are disregarded. The threshold π_{thr} is a tuning parameter but its influence is small and sensible values (e.g., $\pi_{thr} \in (0.6, 0.9)$) tend to give similar results.

2.6 Model Equivalence

There is one further subtlety that makes our approach for finding stable models (or sub-models) slightly more complicated than that in [24]. If we find a particular model, we have to account for the fact that there may be different models that are observationally indistinguishable. Causal models represented by DAGs have their corresponding model equivalent classes, called *Completed Partially Directed Acyclic Graph* (CPDAG). This means that every probability distribution derived from a model in a particular CPDAG, can also be derived by models belonging to the same CPDAG. In SEMs, these models are called covariance equivalent [2].

The characterization of equivalent structures is given by the following theorem [25].

Theorem 1. (Verma and Pearl, 1990) *Two DAGs are equivalent if and only if they have the same skeletons and the same v -structures.*

Furthermore, a directed edge $x \rightarrow y$ is compelled in \mathcal{G} if for every DAG \mathcal{G}' equivalent to \mathcal{G} , $x \rightarrow y$ exists in \mathcal{G}' . For any edge e in \mathcal{G} , if e is not compelled in \mathcal{G} , then e is reversible. A CPDAG can be represented by a directed edge (arc) for every compelled edge and an undirected edge for every reversible edge [11].

Converting a model into a CPDAG allows one to observe the relations that hold among the variables. Arcs in a CPDAG indicate a cause-effect relation among variables since the

same arc occurs in all members of the CPDAG. Undirected edges $A - B$ in a CPDAG indicate that some members of the CPDAG contain an arc $A \rightarrow B$ whereas other members contain an arc $B \rightarrow A$.

3 PROPOSED METHOD

3.1 The General Idea

Our proposed method generally can be divided into two phases. The first phase is *search* and the second phase is *visualization*. In the search phase SEM and NSGA-II are synergically combined for exploratory search of the model space. As portrayed in Figure 4, the *inner loop* is an iterative process, searching over the model space and returns a Pareto front of models. The *outer loop* is an iterative process that samples a different subset of the data in each iteration and at the end returns a number of Pareto fronts coming from those subsets. Each model returned by the outer loop is transformed into a CPDAG which are then used to compute the *edge stability graph* and the *causal path stability graph*.

Definition 4. (*Stability graphs*) Let A and B be two variables and G a multiset (or bag) of CPDAGS. Let G_c be the submultiset of G containing all CPDAGS with complexity c . The edge

stability for A and B at complexity c is the number of models in G_c for which there exists an edge between A and B (i.e., $A \rightarrow B$, $B \rightarrow A$, or $A - B$) divided by the total number of models in G_c . The causal path stability for A to B at complexity c is the number of models in G_c for which there is a directed path from A to B (of any length) divided by the total number of models in G_c . The terms *edge stability graph* and *causal path stability graph* are used to denote the corresponding measures for all variable pairs and all complexity levels.

On top of the stability graphs we perform stability selection. In [24], stability selection is defined in terms of a regularization parameter λ . In our approach we do not have a regularization parameter and instead use model complexity (defined in Section 4.1) which is one of the objectives in our multi-objective optimization approach. We therefore define two thresholds. The first threshold is the boundary of occurrence π_{occ} and corresponds to π_{thr} in [24]. For example, setting $\pi_{\text{occ}} = 0.6$ means that all causal relationships with edge stability or causal path stability (Figure 5) above this threshold are considered *stable*. The second threshold is the boundary of complexity π_{bic} , which is used to control overfitting and corresponds to minimal λ in [24]. We set π_{bic} to the level of model complexity at which the minimum average *Bayesian Information Criterion* (BIC) score is found. For example, $\pi_{\text{bic}} = 7$ means that all causal relationships with an edge stability or a causal path stability lower than this threshold (Figure 5) are considered *parsimonious*. Causal relationships that intersect with the top-left region are considered both *stable* and *parsimonious* and called *relevant*.

In the visualization phase we combine the stability graphs into a graph with nodes and edges. This is done by adding the relevant edges and orienting them using background knowledge (Section 3.2) and the relevant causal paths. This visualization eases interpretation but the stability graphs are considered to be the main outcome of our approach.

3.2 Constrained SEM

In practise, one often has prior knowledge about the domain, for example, that A does

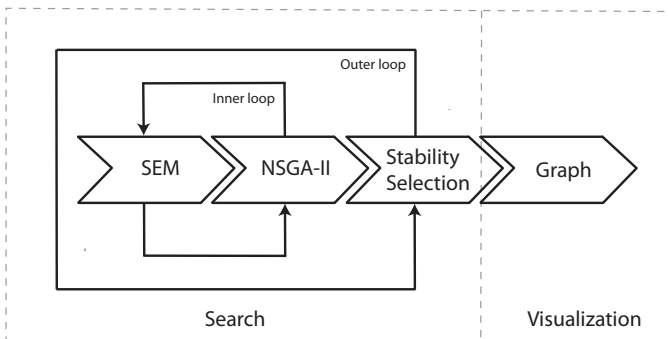


Fig. 4: The proposed method consists of two phases: *search* and *visualization*. The search phase is an iterative process using an *outer loop* and *inner loop* that combines SEM, NSGA-II, and stability selection. The output of this phase are the relevant edges and causal paths between two variables. The visualization phase displays the relevant relationships as a causal model.

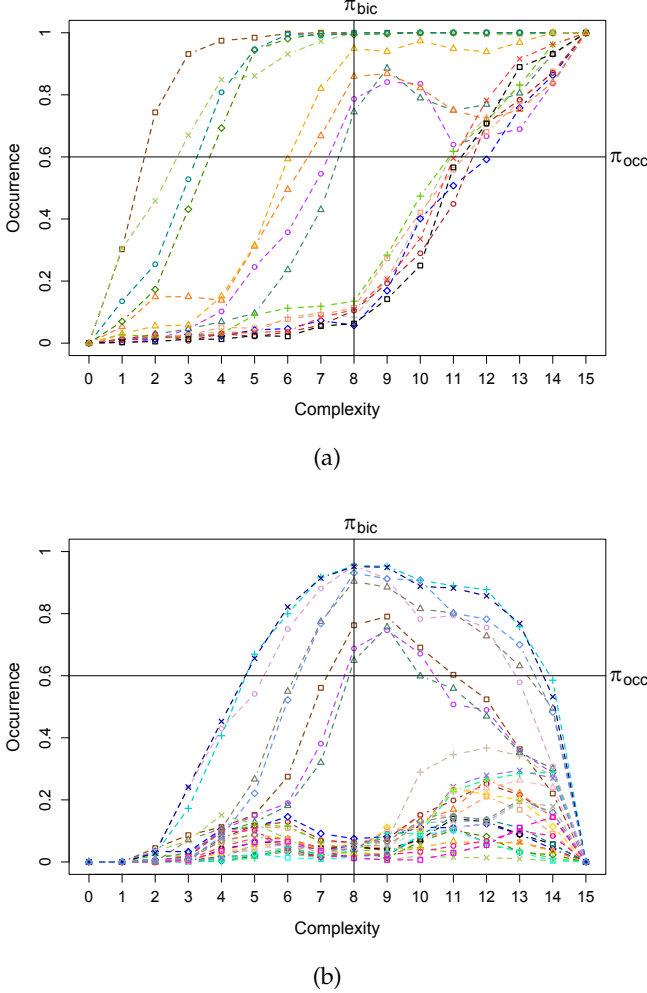


Fig. 5: An example of stability graphs from an artificial data set of 400 instances with six continuous variables, without prior knowledge. (a) Edge stability graph. (b) Causal path stability graph.

not cause B directly, denoted by $A \not\rightarrow B$. The method proposed here can include such prior knowledge, extending previous work [26], since this translates to a DAG with no directed edge from A to B .¹

Model specifications should comply with any prior knowledge when performing specification search and when measuring the edge and causal path stability. When DAGs are converted into CPDAGs in the outer loop, a constraint $A \not\rightarrow B$ may be violated since arcs $B \rightarrow A$ in the DAG may be converted

into undirected (reversible) edges $A - B$ in the CPDAG. In order to preserve constraints we therefore extended the efficient DAG-TO-CPDAG algorithm of [11] which runs in time $\mathcal{O}(|E|)$ given a DAG $G = (V, E)$.

Figure 6 provides pseudocode for the constrained DAG to CPDAG algorithm. Line 2 produces a total ordering E' over the edges in DAG G . Lines 3-6 impose an arc upon the edges that match the constraints. Finally, Line 7 uses [11] to label the remaining edges $E \setminus E'$ in G with “compelled” or “reversible” and returns the constrained CPDAG G' .

A DAG without edges will always be transformed into a CPDAG without edges. A fully connected DAG without constraints will be transformed into a CPDAG with only undirected edges. However, if background knowledge is added, a fully connected DAG will be transformed into a CPDAG in which the edges corresponding to the background knowledge are directed. From these observations it follows that in the edge stability graph all paths start with a selection probability of 0 and end up in a selection probability of 1. In the causal path stability graph when no prior knowledge has been added all paths start with a selection probability of 0 and end up in a selection probability of 1. However, when prior knowledge is added some of the paths may end up in a selection probability of 1 because of the added constraints.

3.3 The Algorithm

Figure 7 provides pseudocode for our approach (cf. Figure 4). Lines 3-18 represent the outer loop, Lines 6-16 represent the inner loops, Lines 19-21 compute the edge and path stability graphs.

An inner loop (Lines 6-16) starts by forming a population P of size N , initially at random, or else from a previous population using crowding distance sorting (Lines 7-12). Line 13 forms a new population Q by manipulating P using tournament selection, crossover, and mutation. Line 14 combines P and Q and sorts them using fast non-dominated sorting. Line 15 updates the Pareto front in F_1 .

An outer loop (Lines 3-18) starts by sampling a subset T from D with size $\lfloor |D|/2 \rfloor$ at random

1. This still allows for directed edges from B to A or indirect relations from A to B .

```

1: function consDag2Cpdag(DAG  $G$ , constraint  $\mathcal{C}$ )
2:    $E' \leftarrow \text{orderEdges}(G)$ 
3:   for every constraint  $c \in \mathcal{C}$  do
4:     get  $e \in E'$  that matches  $c$ 
5:     label  $e$  with "compelled" in the direction consistent with  $c$ 
6:   end for
7:   return  $G' \leftarrow \text{labelEdges}(G, E')$  ▷ label remaining edges using [11]
8: end function

```

Fig. 6: The constrained DAG-TO-CPDAG algorithm returns a CPDAG which is consistent with the added prior knowledge and extends [11]. The algorithm first labels the edges that match the constraints with "compelled" and then labels the remaining edges with "reversible" or "compelled" using [11].

```

1: procedure stableSpecificationSearch(data set  $D$ , constraint  $\mathcal{C}$ )
2:    $H \leftarrow ()$  ▷ initialize
3:   for  $j \leftarrow 0, \dots, J-1$  do ▷  $J$  is number of outer loop iterations
4:      $T \leftarrow$  subset of  $D$  with size  $\lfloor |D|/2 \rfloor$  without replacement
5:      $F_1 \leftarrow ()$  ▷ initialize Pareto fronts to empty list
6:     for  $i \leftarrow 0, \dots, I-1$  do ▷  $I$  is number of inner loop iterations
7:       if  $i = 0$  then
8:          $P \leftarrow N$  random DAGs consistent with  $\mathcal{C}$ 
9:          $P \leftarrow \text{fastNonDominatedSort}(P)$ 
10:      else
11:         $P \leftarrow \text{crowdingDistanceSort}(F)$  ▷ draw the first  $N$  models
12:      end if
13:       $Q \leftarrow$  make population from  $P$ 
14:       $F \leftarrow \text{fastNonDominatedSort}(P \cup Q)$ 
15:       $F_1 \leftarrow$  pareto front of  $F$  and  $F_1$ 
16:    end for
17:     $H \leftarrow H \cup F_1$  ▷ concatenation
18:  end for
19:   $G \leftarrow \text{consDag2Cpdag}(H, \mathcal{C})$ 
20:  edges  $\leftarrow$  edge stability of  $G$ 
21:  paths  $\leftarrow$  path stability of  $G$ 
22: end procedure

```

Fig. 7: Stable specification search consists of an outer and an inner loop. The outer loop samples a subset of the data, and for every subset, the inner loop searches for the Pareto front by applying NSGA-II. The Pareto fronts are converted into constrained CPDAGs which are then used to compute the edge and causal path stability graphs.

(Line 4), runs the inner loop I times to obtain a Pareto front (Lines 6-16), and stores it in H (Line 17). After J iterations, H contains J Pareto fronts.

Lines 19-21 convert the J Pareto fronts in H from DAGs into CPDAGs using the algorithm in Figure 7 and then computes the edge

and causal path stability graphs. The stability graphs are considered to be the main outcome of our approach, but can also be visualized as a graph with nodes and edges.

4 EXPERIMENTAL STUDY

The algorithm was implemented in the R language [27]. We used the *SEM* package [28], [29]; the DAG-TO-CPDAG algorithm from the *pcalg* package modified to handle constraints [30], the *nsga2R* package [31], and several packages for handling matrices and graphs [32], [33].

We evaluated our proposed method on simulated and real-world data sets. For simulated data we generated data from the Waste Incinerator network, and for real-world data we used data sets for *Chronic Fatigue Syndrome* (CFS) and for *Attention Deficit Hyperactivity Disorder* (ADHD). Two data sets contain a mixture of discrete and continuous variables and one data set contains only discrete variables.

4.1 Parameter Settings

For all experiments, we employed the same set of NSGA-II parameters and stability thresholds. Specifically the parameters for NSGA-II were set as follows: the number of generations (inner loop) was 20, the size of the population P was 100, *one-point* crossover with rate 0.85, *1-bit flip* mutation with rate 0.075 and tournament selection (in the initial stage).

We score the models using the *chi-square* χ^2 and the *model complexity*. The χ^2 measures the data fit by the discrepancy between the model covariance matrix and the model-implied covariance matrix. The model complexity represents how many predicted parameters the model contains. Under the assumption that variances of parameters are always predicted, the maximum model complexity with n variables is given by $n(n-1)/2$.

When using multi-objective optimization we minimize both the χ^2 and model complexity objectives. These two objectives are, however, conflicting with each other. For example, minimizing the model complexity typically means compromising the data fit.

The thresholds were set to $\pi_{\text{occ}} = 0.6$ (except for the Waste Incinerator data where we vary π_{occ} to study its effect) and π_{bic} equal to the complexity level at which the minimum average BIC score is obtained. We had 100 iterations in the outer loop, and in each iteration we drew a subsample with size $\lfloor |D|/2 \rfloor$.

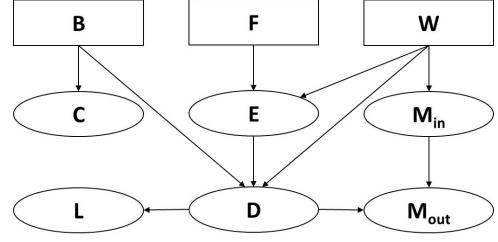


Fig. 8: The Waste Incinerator network consists of nine variables. Rectangular nodes represent discrete variables, oval nodes represent continuous variables, and arcs represent direct causal relations.

4.2 Application to Simulated Data

4.2.1 Data Generation

In this experiment we generated data using the Waste Incinerator network in Figure 8, which is a model of waste emissions from an incinerator plant [34]. This model contains both discrete and continuous random variables, with B the waste burning regimen, W the compositional differences in incoming waste, C the concentration of CO₂, F the filter state, E the filter efficiency, L the light penetrability, D the emission of dust, M_{in} the metals in waste, and M_{out} the metals emission. Following [35], we treat all discrete variables as continuous. We added prior knowledge that none of the variables directly cause the filter state. We generated 1000 samples from this network using the BNT toolbox with the default parameter setting [36].

4.2.2 Performance Measure

Since the true model of the Waste Incinerator data is known, we measure the performance of our method by means of the *Receiver Operating Characteristic* (ROC) curve [37] for both edges and causal paths. We set the threshold π_{occ} to a fixed value ($\pi_{\text{occ}} \in \{0.3, 0.6, 0.8, 0.9\}$) while allowing π_{bic} to vary. The *True Positive Rate* (TPR) and the *False Positive Rate* (FPR) are computed with respect to the CPDAG of the true model. For example, in the case of causal path stability, a true positive means that a causal path obtained through our approach (i.e., lies within the top-left region bounded by the thresholds π_{occ} and π_{bic}) is actually present in the CPDAG of the true model.

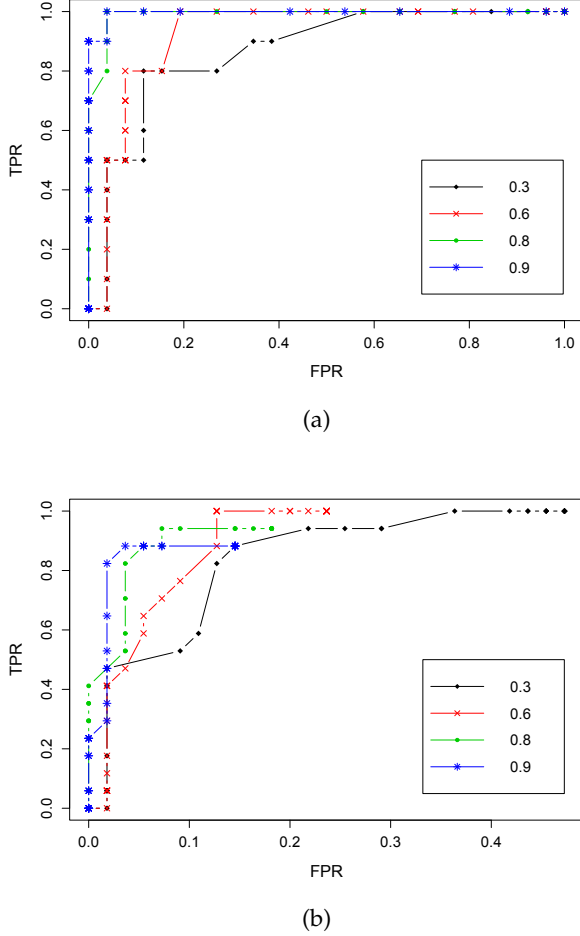


Fig. 9: A plot of ROC curves for (a) the edge stability and (b) the causal path stability, for different values of π_{occ} . A higher π_{occ} shows a better ROC curve. See the main text for an explanation why the ROC curve for causal path stability stops at some point.

4.2.3 Discussion of Waste Incinerator Result

Figure 9 shows the ROC curves for (a) the edge stability, and (b) the causal path stability, for different values of π_{occ} . Higher values for π_{occ} tend to give better ROC curves. This suggests that our approach is able to find the underlying structure with high reliability scores.

As explained in Section 3.2, since all paths in the edge stability graph end up with a selection probability of 1 both the TPR and FPR go all the way up to 1. On the other hand, as some of the paths in the causal path stability graph end up with a selection probability of 0, the corresponding ROC curve cannot reach the up-

per right corner with $TPR = FPR = 1$. Figure 9b shows that when π_{occ} increases the effective range for both the TPR and FPR decreases, because some of the causal paths will then lie entirely below the π_{occ} threshold.

4.3 Application to Real-world Data

This section describes the results of applying our proposed method on two real-world data sets. Both of them are about particular diseases, for which the underlying causal relationships are often not clear. Revealing such causal relationships can lead to the development of (new) dedicated treatments and medications. Here, we consider data on *Attention Deficit Hyperactivity Disorder* (ADHD) and *Chronic Fatigue Syndrome* (CFS).

4.3.1 Performance Measure

Since the true model is unknown we measure the performance of our method using the edge stability and causal path stability graphs. We set the thresholds to $\pi_{occ} = 0.6$ and π_{bic} to the minimum average of BIC scores. The relevant causal relations are those which occur in the top-left region (see Figure 5 as example). We compare the stability graphs to studies reported in the literature.

4.3.2 Application to CFS

In this experiment we consider a data set about *Chronic Fatigue Syndrome* (CFS) of 183 subjects [38]. Originally the data comes from a longitudinal study with five time slices, but in this paper, we focus only on one time slice representing the subjects after the first treatment.

The data set contains six discrete variables; fatigue severity assessed with the subscale fatigue severity of the Checklist Individual Strength (CIS), the sense of control over fatigue assessed with the *self-efficacy scale* (SES), focusing on symptoms measured with the *Illness Management Questionnaire*, the objective activity of the patient measured using an *actometer* (oActivity), the subject's perceived activity measured with the subscale activity of the CIS (pActivity), and physical functioning measured with subscale physical functioning of the *medical outcomes survey* (SF36). We refer to the original paper [38], for a detailed description of the

questionnaires used and the actometer. Missing values were imputed using an imputation method *Expectation Maximization* implemented in SPSS [39]. As all of the variables have large scales, e.g., in the range between 0 to 155, we treat them as continuous variables. We added prior knowledge that the variable fatigue does not cause any of the other variables directly.

Figure 10 shows that eight relevant edges were found. These edges are between pActivity and fatigue, focusing and fatigue, functioning and fatigue, control and fatigue, pActivity and focusing, pActivity and oActivity, focusing and control, and functioning and control. Figure 10 shows that four relevant causal paths were found. These causal paths are: pActivity to fatigue, control to fatigue, functioning to fatigue, and focusing to fatigue.

The stability graphs can be combined into a model as follows. First, the nodes are connected according to the eight relevant edges obtained. Second, the edges are oriented according to the background knowledge added. The fact that the variable fatigue does not directly cause any other variable results in four directed edges, which, in this case, correspond exactly to the relevant causal paths obtained. The inferred model is shown in Figure 11. Each edge is annotated with a reliability score which is the maximum score obtained in the top-left region of the edge stability graph.

A (direct) causal path $X \rightarrow Y$ in Figure 11 indicates that a change in variable X causes a change in variable Y . All variables except for objective activity were found to be direct causes for fatigue severity, which are corroborated by studies reported in the literature. In [40], changes in physical activity, sense of control, and focus on the symptoms measured, were shown to result in changes in fatigue. In [41], changes in perceived activity, sense of control, and physical functioning were shown to result in changes in the fatigue. In [38], an increase in sense of control, perceived activity, and self-reported physical functioning, as well as a decrease in focusing on symptoms resulted in a decrease of fatigue, whereas changes in objective activity did not result in any change in the fatigue.

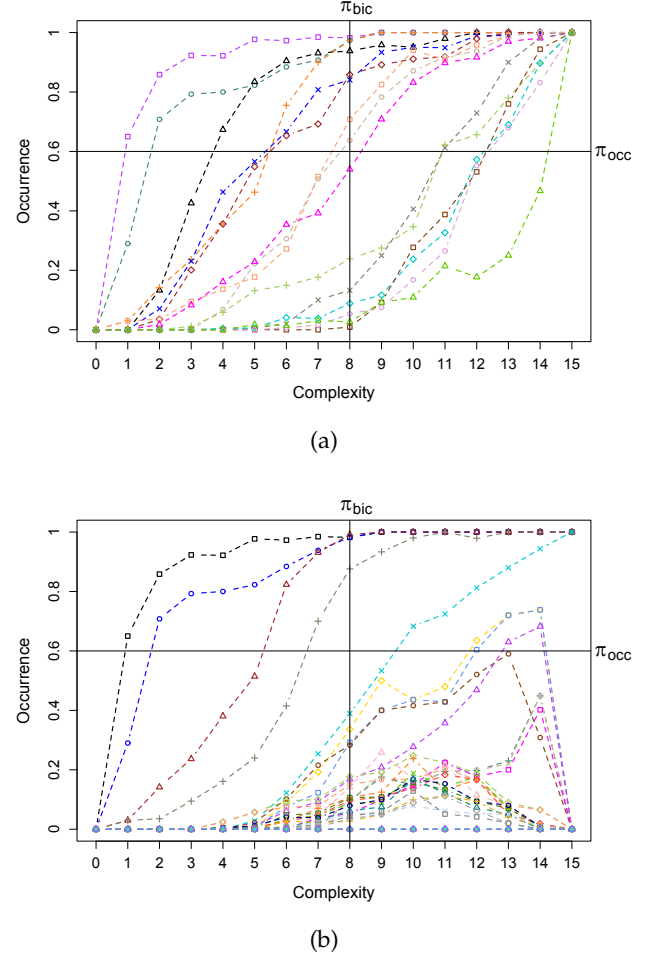


Fig. 10: The stability graphs for CFS together with π_{occ} and π_{bic} , yielding four regions. The top-left region is the area containing the relevant causal relations. (a) The edge stability graph showing eight relevant edges. (b) The causal path stability graph showing four relevant causal paths. For a further detail of to which edges or causal paths the lines correspond, see Tables 1 and 2 in Appendix A.

4.3.3 Application to ADHD

In this experiment we consider a data set about *Attention Deficit Hyperactivity Disorder* (ADHD) of 245 subjects with 23 variables [42]. Following [43], we excluded instances with missing values and variables that either have insufficient instances or are considered irrelevant. The remaining data set consists of 221 instances and six variables with gender the gender of subjects, AD the attention deficit measure, HI the assessment of hyperactivity/impulsivity symptoms,

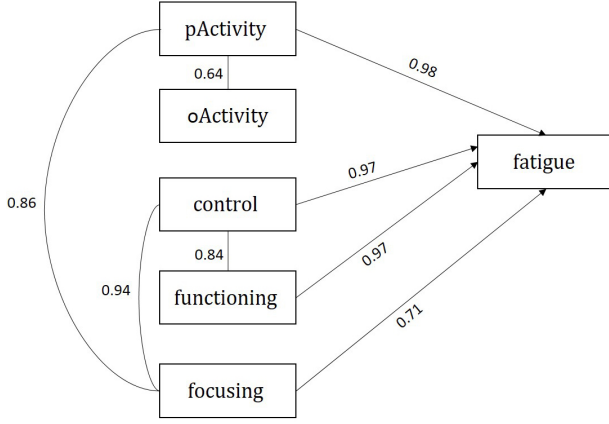


Fig. 11: The inferred model of CFS by combining the edge stability and causal path stability graphs. Each edge has a reliability score which is the maximum score obtained in the top-left region of the edge stability graph.

aggression the measure of aggressive behavior, medication the medication status of subjects, and handedness represents whether a subject uses the right and/or left hand. Following [35], we treat all discrete variables as continuous variables. We added prior knowledge that the variable gender does not cause any of the other variables directly.

Figure 12 shows that there are four relevant edges, namely between gender and AD, AD and medication, AD and HI, and HI and aggression. Moreover, Figure 12 shows that there are seven relevant causal paths; gender to AD, gender to HI, gender to medication, gender to aggression, AD to HI, AD to medication, and AD to aggression.

The stability graphs can be combined into a model as follows. First, the nodes are connected according to the four relevant edges obtained. Second, the edges are oriented according to the background knowledge added. The fact that the variable gender does not directly cause any other variable results in one directed edge $\text{gender} \rightarrow \text{AD}$. Third, the edges are oriented according to the relevant causal paths obtained. This results in two directed edges, $\text{AD} \rightarrow \text{HI}$ and $\text{AD} \rightarrow \text{medication}$. Since there is no relevant edge between AD and aggression and no relevant causal path from HI to aggression we cannot orient any other edges and therefore cannot represent two of the relevant causal

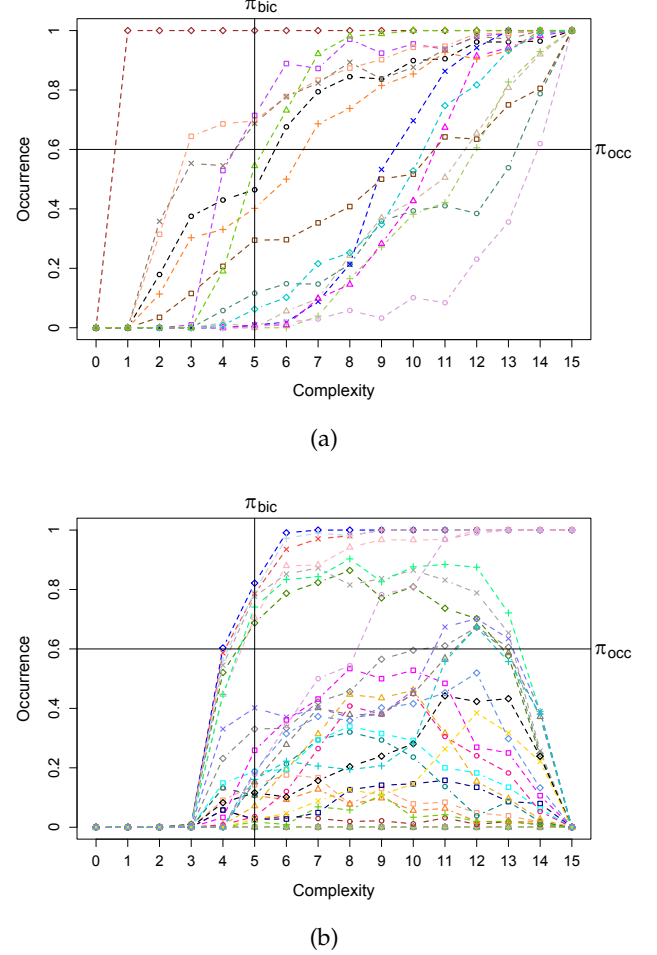


Fig. 12: The stability graphs for ADHD together with π_{occ} and π_{bic} , yielding four regions. The top-left region is the area containing the relevant causal relations. (a) The edge stability graph showing four relevant edges. (b) The causal path stability graph showing seven relevant causal paths. For a further detail of to which edges or causal paths the lines correspond, see Tables 3 and 4 in Appendix A.

paths in the model. We lose some information when converting the stability graphs into a model. The inferred model is shown in Figure 13. Each label is annotated with a reliability score which is the maximum score obtained in the top-left region of the edge stability graph.

The causal relations obtained for ADHD are corroborated by studies reported in the literature. In [43], gender is shown to be a direct cause for attention deficit, attention deficit is shown to be a direct cause for both hyperac-

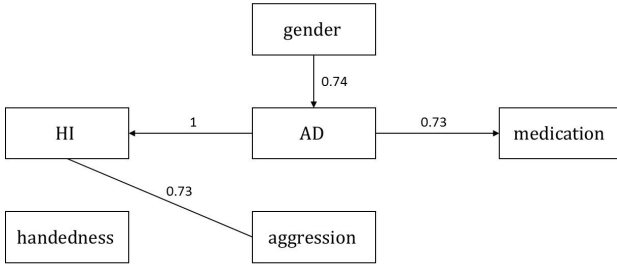


Fig. 13: The inferred model of ADHD by combining the edge stability and causal path stability graphs. Each edge has a reliability score which is the maximum score obtained in the top-left region of the edge stability graph.

tivity, medication, and aggression, and hyperactivity and aggression are related but neither variable is a direct cause for the other.

5 CONCLUSION AND FUTURE WORK

In the last decades the field of causal modeling has seen a surge in theoretical development and the construction of various causal discovery algorithms. In general, discovery algorithms can be divided into two approaches: constraint-based and score-based. A disadvantage, however, of currently existing discovery algorithms is the inherent instability of structure estimation. With finite samples small changes in the data can lead to completely different optimal structures.

The present work introduces a new score-based discovery algorithm that is robust for finite samples based on subsampling and selection algorithms. Our approach uses exploratory search to search over Structural Equation Models and allows incorporation of prior background knowledge. Experimental results on both artificial and real-world data sets show that our method is able to obtain reliable structure estimates.

Several issues have not yet been explored in our current approach that warrant further research: latent variables and longitudinal data. Taking into account the existence of latent variables can further improve our structure estimate by properly identifying dependencies between variables as an unmeasured common cause acting on both variables. In longitudinal

data several subjects are measured at different time slices which provides a richer structure that can be incorporated in the causal discovery algorithm.

APPENDIX A

TABLE 1: Edge stability of CFS

Lines	Edges
□- - - - □- - - - □	fatigue and pActivity
○- - - - ○- - - - ○	fatigue and control
△- - - - △- - - - △	control and focusing
+ - - - - + - - - - +	fatigue and functioning
×- - - - ×- - - - ×	control and functioning
◇- - - - ◇- - - - ◇	focusing and pActivity
□- - - - □- - - - □	fatigue and focusing
○- - - - ○- - - - ○	pActivity and oActivity
△- - - - △- - - - △	functioning and pActivity
+ - - - - + - - - - +	control and pActivity
×- - - - ×- - - - ×	control and oActivity
◇- - - - ◇- - - - ◇	focusing and oActivity
□- - - - □- - - - □	fatigue and oActivity
○- - - - ○- - - - ○	functioning and oActivity
△- - - - △- - - - △	functioning and focusing

TABLE 2: Causal path stability of CFS

Lines	Causal Paths
□- - - - □- - - - □	pActivity to fatigue
○- - - - ○- - - - ○	control to fatigue
△- - - - △- - - - △	functioning to fatigue
+ - - - - + - - - - +	focusing to fatigue
×- - - - ×- - - - ×	oActivity to fatigue
◇- - - - ◇- - - - ◇	focusing to pActivity
□- - - - □- - - - □	functioning to pActivity
○- - - - ○- - - - ○	oActivity to pActivity
△- - - - △- - - - △	control to pActivity
+ - - - - + - - - - +	functioning to oActivity
×- - - - ×- - - - ×	focusing to oActivity
◇- - - - ◇- - - - ◇	focusing to control
□- - - - □- - - - □	control to oActivity
○- - - - ○- - - - ○	functioning to control
△- - - - △- - - - △	pActivity to oActivity
+ - - - - + - - - - +	control to functioning
×- - - - ×- - - - ×	oActivity to functioning
◇- - - - ◇- - - - ◇	oActivity to control
□- - - - □- - - - □	oActivity to focusing
○- - - - ○- - - - ○	control to focusing
△- - - - △- - - - △	pActivity to functioning
+ - - - - + - - - - +	focusing to focusing
×- - - - ×- - - - ×	pActivity to control
◇- - - - ◇- - - - ◇	pActivity to focusing
□- - - - □- - - - □	fatigue to pActivity
○- - - - ○- - - - ○	fatigue to oActivity
△- - - - △- - - - △	fatigue to focusing
+ - - - - + - - - - +	fatigue to functioning
×- - - - ×- - - - ×	fatigue to control
◇- - - - ◇- - - - ◇	

TABLE 3: Edge stability of ADHD

Lines	Edges
◇-----◇-----◇	AD and HI
□-----□-----□	AD and medication
×-----×-----×	HI and aggression
◇-----◇-----◇	gender and AD
○-----○-----○	aggression and AD
+-----+-----+	AD and medication
△-----△-----△	handedness and aggression
□-----□-----□	medication and aggression
○-----○-----○	gender and HI
◇-----◇-----◇	HI and handedness
△-----△-----△	gender and medication
×-----×-----×	gender and handedness
△-----△-----△	AD and handedness
+-----+-----+	gender and aggression
○-----○-----○	medication and handedness

TABLE 4: Causal path stability of ADHD

Lines	Causal Paths
◇-----◇-----◇	gender to AD
×-----×-----×	gender to HI
+-----+-----+	gender to medication
×-----×-----×	AD to medication
◇-----◇-----◇	AD to HI
+-----+-----+	AD to aggression
△-----△-----△	gender to aggression
×-----×-----×	HI to aggression
◇-----◇-----◇	HI to medication
□-----□-----□	aggression to medication
○-----○-----○	aggression to HI
□-----□-----□	HI to AD
◇-----◇-----◇	medication to aggression
□-----□-----□	handedness to aggression
○-----○-----○	gender to handedness
◇-----◇-----◇	aggression to handedness
△-----△-----△	AD to handedness
+-----+-----+	HI to handedness
△-----△-----△	handedness to HI
○-----○-----○	handedness to medication
□-----□-----□	medication to HI
△-----△-----△	aggression to gender
×-----×-----×	medication to handedness
+-----+-----+	aggression to HI
○-----○-----○	medication to AD
□-----□-----□	AD to gender
○-----○-----○	HI to gender
△-----△-----△	medication to gender
+-----+-----+	aggression to gender
×-----×-----×	handedness to gender

ACKNOWLEDGMENTS

The research leading to these results has received funding from the DGHE of Indonesia and the European Community's Seventh Framework Programme (FP7/2007-2013) under grant agreement n° 305697.

REFERENCES

- [1] B. van Engelen *et al.*, "Cognitive behaviour therapy plus aerobic exercise training to increase activity in patients with myotonic dystrophy type 1 (dm1) compared to usual care (optimistic): study protocol for randomised controlled trial," *Trials*, vol. 16, no. 1, p. 224, 2015.
- [2] J. Pearl, *Causality: models, reasoning and inference*. Cambridge Univ Press, 2000, vol. 29.
- [3] J. Pearl, T. Verma *et al.*, *A theory of inferred causation*. Morgan Kaufmann San Mateo, CA, 1991.
- [4] P. Spirtes, C. N. Glymour, and R. Scheines, *Causation, prediction, and search*. MIT press, 2000, vol. 81.
- [5] J.-P. Pellet and A. Elisseeff, "Using markov blankets for causal structure learning," *The Journal of Machine Learning Research*, vol. 9, pp. 1295–1342, 2008.
- [6] A. P. Dawid, "Present position and potential developments: Some personal views: Statistical theory: The prequential approach," *Journal of the Royal Statistical Society. Series A (General)*, pp. 278–292, 1984.
- [7] G. Schwarz *et al.*, "Estimating the dimension of a model," *The annals of statistics*, vol. 6, no. 2, pp. 461–464, 1978.
- [8] P. Spirtes, "Introduction to causal inference," *The Journal of Machine Learning Research*, vol. 11, pp. 1643–1662, 2010.
- [9] J. Ramsey, J. Zhang, and P. L. Spirtes, "Adjacency-faithfulness and conservative causal inference," *arXiv preprint arXiv:1206.6843*, 2012.
- [10] P. Spirtes, C. Glymour, and R. Scheines, "The tetrad project: Causal models and statistical data," 2006.
- [11] D. M. Chickering, "Learning equivalence classes of Bayesian-network structures," *The Journal of Machine Learning Research*, vol. 2, pp. 445–498, 2002.
- [12] R. MacCallum, "Specification searches in covariance structure modeling," *Psychological Bulletin*, vol. 100, no. 1, p. 107, 1986.
- [13] E. E. Leamer, *Specification searches: Ad hoc inference with nonexperimental data*. Wiley New York, 1978.
- [14] J. S. Long, *Covariance structure models: An introduction to LISREL*. Sage, 1983, no. 34.
- [15] G. A. Marcoulides, Z. Drezner, and R. E. Schumacker, "Model specification searches in structural equation modeling using tabu search," *Structural Equation Modeling: A Multidisciplinary Journal*, vol. 5, no. 4, pp. 365–376, 1998.
- [16] G. A. Marcoulides and Z. Drezner, "Specification searches in structural equation modeling with a genetic algorithm," *New developments and techniques in structural equation modeling*, pp. 247–268, 2001.
- [17] H. Murohashi and H. Toyoda, "Model specification search using a genetic algorithm with factor reordering for a simple structure factor analysis model," *Japanese Psychological Research*, vol. 49, no. 3, pp. 179–191, 2007.
- [18] G. A. Marcoulides and Z. Drezner, "Model specification searches using ant colony optimization algorithms," *Structural Equation Modeling: A Multidisciplinary Journal*, vol. 10, no. 1, pp. 154–164, 2003.
- [19] J. Herting and H. Costner, "Respecification in multiple indicator models," *Causal Models in the Social Sciences*, pp. 321–393, 1985.
- [20] P. Spirtes, R. Scheines, and C. Glymour, "Simulation studies of the reliability of computer-aided model specification using the TETRAD II, EQS, and LISREL programs," *Sociological Methods & Research*, vol. 19, no. 1, pp. 3–66, 1990.
- [21] W. E. Saris, A. Satorra, and D. Sörbom, "The detection and correction of specification errors in structural equation models," *Sociological methodology*, vol. 17, pp. 105–129, 1987.

- [22] K. Deb, *Multi-objective optimization using evolutionary algorithms*. John Wiley & Sons Chichester, 2001, vol. 2012.
- [23] K. Deb, A. Pratap, S. Agarwal, and T. Meyarivan, "A fast and elitist multiobjective genetic algorithm: NSGA-II," *IEEE Transactions on Evolutionary Computation*, vol. 6, no. 2, pp. 182–197, 2002.
- [24] N. Meinshausen and P. Bühlmann, "Stability selection," *Journal of the Royal Statistical Society: Series B (Statistical Methodology)*, vol. 72, no. 4, pp. 417–473, 2010.
- [25] T. Verma and J. Pearl, "Equivalence and synthesis of causal models," in *Proceedings of the Sixth Annual Conference on Uncertainty in Artificial Intelligence*. Elsevier Science Inc., 1990, pp. 255–270.
- [26] R. Rahmadi, P. Groot, and T. Heskes, "Stable specification searches in structural equation modeling using multi-objective evolutionary algorithm," in *Proceedings of SNATI*, 2014.
- [27] R Core Team, *R: A Language and Environment for Statistical Computing*, R Foundation for Statistical Computing, Vienna, Austria, 2013. [Online]. Available: <http://www.R-project.org/>
- [28] J. Fox, Z. Nie, and J. Byrnes, *SEM: Structural Equation Models*, 2014, R package version 3.1-4. [Online]. Available: <http://CRAN.R-project.org/package=sem>
- [29] J. Fox, "Teacher's corner: structural equation modeling with the sem package in R," *Structural equation modeling*, vol. 13, no. 3, pp. 465–486, 2006.
- [30] M. Kalisch, M. Mächler, D. Colombo, M. H. Maathuis, and P. Bühlmann, "Causal inference using graphical models with the R package pcalg," *Journal of Statistical Software*, vol. 47, no. 11, pp. 1–26, 2012. [Online]. Available: <http://www.jstatsoft.org/v47/i11/>
- [31] C.-S. Tsou, *nsga2R: Elitist Non-dominated Sorting Genetic Algorithm based on R*, 2013, R package version 1.0. [Online]. Available: <http://CRAN.R-project.org/package=nsga2R>
- [32] F. Novomestky, *matrixcalc: Collection of functions for matrix calculations*, 2012, R package version 1.0-3. [Online]. Available: <http://CRAN.R-project.org/package=matrixcalc>
- [33] R. Gentleman, E. Whalen, W. Huber, and S. Falcon, *graph: A package to handle graph data structures*, R package version 1.40.1.
- [34] S. L. Lauritzen, "Propagation of probabilities, means, and variances in mixed graphical association models," *Journal of the American Statistical Association*, vol. 87, no. 420, pp. 1098–1108, 1992.
- [35] M. Rhemtulla, P. É. Brosseau-Liard, and V. Savalei, "When can categorical variables be treated as continuous? a comparison of robust continuous and categorical sem estimation methods under suboptimal conditions," *Psychological methods*, vol. 17, no. 3, p. 354, 2012.
- [36] K. Murphy *et al.*, "The Bayes Net Toolbox for Matlab," *Computing science and statistics*, vol. 33, no. 2, pp. 1024–1034, 2001.
- [37] T. Fawcett, "ROC graphs: Notes and practical considerations for researchers," *Machine learning*, vol. 31, pp. 1–38, 2004.
- [38] M. J. Heins, H. Knoop, W. J. Burk, and G. Bleijenberg, "The process of cognitive behaviour therapy for chronic fatigue syndrome: Which changes in perpetuating cognitions and behaviour are related to a reduction in fatigue?" *Journal of psychosomatic research*, vol. 75, no. 3, pp. 235–241, 2013.
- [39] *IBM SPSS Statistics for Windows, Version 19.0.*, IBM Corp., Armonk, NY, 2010.
- [40] J. Vercoulen, C. Swanink, J. Galama, J. Fennis, P. Jongen, O. Hommes, J. Van der Meer, and G. Bleijenberg, "The persistence of fatigue in chronic fatigue syndrome and multiple sclerosis: development of a model," *Journal of psychosomatic research*, vol. 45, no. 6, pp. 507–517, 1998.
- [41] J. F. Wiborg, H. Knoop, L. E. Frank, and G. Bleijenberg, "Towards an evidence-based treatment model for cognitive behavioral interventions focusing on chronic fatigue syndrome," *Journal of psychosomatic research*, vol. 72, no. 5, pp. 399–404, 2012.
- [42] Q. Cao, Y. Zang, L. Sun, M. Sui, X. Long, Q. Zou, and Y. Wang, "Abnormal neural activity in children with attention deficit hyperactivity disorder: a resting-state functional magnetic resonance imaging study," *Neuroreport*, vol. 17, no. 10, pp. 1033–1036, 2006.
- [43] E. Sokolova, P. Groot, T. Claassen, and T. Heskes, "Causal discovery from databases with discrete and continuous variables," in *Probabilistic Graphical Models*. Springer, 2014, pp. 442–457.